Supporting Information

Small Molecules of Chalcone Derivative with High Two-photon Absorption Activities in the Near-IR Region

Jingyun Tan,†[a] Yujin Zhang,†[c] Meirong Zhang,[a] Xiaohe Tian,[d] Yiming Wang,[a] Shengli Li,[a] Chuankui Wang,[c] Hongping Zhou,[a] Jiaxiang Yang,[a] Yupeng Tian,[a,b,*] Jieying Wu[a,*]

[a]*Department of Chemistry, Key Laboratory of Functional Inorganic Materials Chemistry of Anhui Province, Anhui University, Hefei 230601, P. R. China;*

[b]*State Key Laboratory of Coordination Chemistry, Nanjing University, Nanjing 210093, P. R. China;*

[c]*College of Physics and Electronics, Shandong Normal University, Jinan 20014, P. R. China;*

[d]*School of life science, Anhui University, Hefei 230601, P. R. China.*

(* Corresponding author: *e-mail: yptian@ahu.edu.cn; jywu1957@163.com*)

†These authors contributed equally to this work

S1. General methods

Crystallography

The X-ray diffraction measurements were performed on a Bruker SMART CCD area detector using graphite monochromated Mo-K_α radiation (λ = 0.71069 Å) at 298(2)K. Intensity data were collected in the variable ω-scan mode. The structures were solved by direct methods and difference Fourier syntheses. The non-hydrogen atoms were refined anisotropically and hydrogen atoms were introduced geometrically. Calculations were performed with SHELXTL-97 program package.[1-2]

TD-DFT studies for linear absorption behaviors

Optimizations were carried out with B3LYP/6-311+G(d) without any symmetry restraint. All calculations, including optimizations and TD-DFT, were performed with the Gaussian03 software.[3] Geometry optimization of the singlet ground state and the TD-DFT calculation of the lowest 30 singlet-singlet excitation energies were calculated

with a basis set composed of 6-311+G(d) for C, H, N, O and S atoms. The basis set was downloaded from the EMSL basis set library. The lowest 25-spin allowed singlet-singlet transitions, up to energy of about 5 eV, were taken into account for the calculation of the absorption spectra.

Linear optical measurements

UV-vis absorption spectra were recorded on a UV-265 spectrophotometer. The one-photon excited fluorescence (OPEF) measurements were carried out on a Hitachi F-7000 fluorescence spectrophotometer. All the spectra were collected at the concentration of 1.0×10^{-5} mol/L. The fluorescence quantum yields (Φ) were determined by using determined using quinine sulfate as the reference according to the literature method.[4] Quantum yields were corrected as follows[4]:

$$\Phi_s = \Phi_r \left(\frac{A_r(\lambda_r)}{A_s(\lambda_s)} \right) \left(\frac{n_s^2}{n_r^2} \right) \frac{\int F_s}{\int F_r} \quad (1)$$

Where the *s* and *r* indices designate the sample and reference samples, respectively, *A* is the absorbance at λ_{exc}, η is the average refractive index of the appropriate solution, and *D* is the integrated area under the corrected emission spectrum. For time-resolved fluorescence measurements, the fluorescence signals were collimated and focused onto the entrance slit of a mono-chromator with the output plane equipped with a photomultiplier tube (HORIBA HuoroMax-4P). The decays were analyzed by 'least-squares'. The quality of the exponential fits was evaluated by the goodness of fit (χ^2).

Two-photon excited fluorescence spectroscopy and DFT studies

2PA cross-sections (δ) of the samples were obtained by the two-photon excited fluorescence (2PEF) method with a femtosecond laser pulse and a Ti:sapphire system (680–1080 nm, 80 MHz, 140 fs) as the light source. The concentration of sample solution was 1.0×10^{-3} M. Thus, the δ values of samples were determined by the following Equation:[5]

$$\delta_s = \delta_r \frac{\Phi_r}{\Phi_s} \frac{c_r}{c_s} \frac{n_r}{n_s} \frac{F_s}{F_r} \quad (2)$$

Where the subscripts "s" and "r" represent sample and reference, respectively. F is the overall fluorescence collection efficiency intensity of the fluorescence signal collected by the fiber spectra meter. Φ, *n* and *c* are the quantum yield of the fluorescence, the refractive index of solvent, and the concentration of the solution, respectively. All measurements were carried out in air at room temperature. Here, fluorescein (38 GM) at a concentration of 1.0×10^{-3} mol/L was used as reference of 2PA cross-sections.[6]

Two-photon absorption cross-section which can be directly comparable with experimental results is defined as follows,

$$\sigma_{2PA} = \frac{4\pi^2 a_0^5 \alpha}{15 c_0} \times \frac{\omega^2 g(\omega)}{\Gamma_f} \delta_{2PA} \qquad (3)$$

Here α_0 is the Bohr radius, c_0 is the speed of light, α is the fine structure constant, ω is the photon frequency of the incident light, and $g(\omega)$denotes the spectral line profile, which is assumed to be a δ function here, Γ_f is the lifetime broadening of the final state, which is commonly assumed to be 0.1 eV,[7] and δ_{2PA} is orientation average value of the two-photon absorption probability, which is written as follows,[8]

$$\delta_{2PA} = \sum_{\alpha\beta} \left[F \times S_{\alpha\alpha} \times S^*_{\beta\beta} + G \times S_{\alpha\beta} \times S^*_{\alpha\beta} + H \times S_{\alpha\beta} \times S^*_{\beta\alpha} \right] \qquad (4)$$

Where F, G, and H are coefficients dependent on the polarization of the light. $S_{\alpha\beta}$ is the two-photon transition matrix element. For the absorption of two photons with the same frequency $\omega_f/2$ it can be written as,[9]

$$S_{\alpha\beta} = \sum_i \left[\frac{\langle 0|\mu_\alpha|i\rangle\langle i|\mu_\beta|f\rangle}{\omega_i - \omega_f/2} + \frac{\langle 0|\mu_\beta|i\rangle\langle i|\mu_\alpha|f\rangle}{\omega_i - \omega_f/2} \right] \qquad (5)$$

where ω_i and ω_f denote the excitation frequency of the intermediate state $|\, i \,\rangle$ and final state $|\, f \,\rangle$ respectively, α, β ∈ (x, y, z), and the summation goes over all the intermediate states including the ground state $|\, 0 \,\rangle$ and the final state $|\, f \,\rangle$.

The most straightforward approach to analyze optical properties of molecules is the response theory,[10] which can provide an analytical solution for the 2PA cross-section. The equilibrium geometries of molecules in the gas phase are optimized based on density functional theory (DFT) with Becke's three parametrized Lee-Yang-Parr (B3LYP) exchange functional and 6-31G(d) basis set by employing the Gaussian09

package.[11] The 2PA properties are calculated by use of the response theory at the DFT level implemented in Dalton quantum chemistry program.[12]

Cell image

HepG2 cells were seeded in 6 well plates at a density of 2x105 cells per well and grown for 96 hours. For live cell imaging cell cultures were incubated with the complexes (10% PBS: 90% cell media) at the concentrations of 40 μM and maintained at 37°C in an atmosphere of 5% CO_2 and 95% air for indicated incubation times ranging for 2 hours. The cells were then washed with PBS (3 x 3 ml per well) and 3 ml of PBS was added to each well.

The cells were imaged on a Zeiss LSM 710 META upright confocal laser scanning microscope using magnification 40× and 100× water-dipping lenses for monolayer cultures. Image data acquisition and processing was performed using Zeiss LSM Image Browser, Zeiss LSM Image Expert and Image J.

S2. Characterization

C-1: M.p.= 152 ^{o}C. ^{1}H-NMR (d_6-acetone, 400 MHz, ppm) δ= 6.47 (d, *J*= 4.8 Hz, 1H), 7.24 (t, *J*= 7.2 Hz, 2H), 7.30 (d, *J*= 8.0 Hz, 4H), 7.35 (d, *J*=4.8 Hz, 1H), 7.43 (d, *J*=8.0 Hz, 4H), 7.59 (t, *J*=6.4 Hz, 1H), 7.76(d, *J*=15.2 Hz, 1H), 7.92 (d, *J*=15.2 Hz, 1H), 7.98(t, *J*=7.6 Hz, 1H), 8.10 (d, *J*=7.6 Hz, 1H), 8.69(d, *J*=4.8 Hz, 1H). ^{13}C-NMR (d_6-acetone, 150 MHz): δ=120.36, 123.80, 125.75, 128.33, 129.48, 129.57, 136.25, 136.30, 136.70, 150.80, 151.32, 155.41, 160.46, 183.78. IR (KBr, cm^{-1}): 3428(w), 3057(w), 1648(m), 1586(s), 1565(s), 1522(s), 1490(m), 1440(vs), 1378(m), 1331(s), 1289(m), 1236(m), 1047(m), 1028(s), 758(m), 699(s). MALDI-TOF: *m/z*, *cal*: 382.11, found: 382.78 [M^{+}].

C-2: M.p.= 119 ^{o}C. ^{1}H-NMR (d_6-acetone, 400 MHz, ppm) δ= 6.47 (d, *J*= 4.8 Hz, 1H), 7.24 (t, *J*= 7.2 Hz, 2H), 7.30 (d, *J*= 8.0 Hz, 4H), 7.35 (d, *J*=4.8 Hz, 1H), 7.43 (d, *J*=8.0 Hz, 4H), 7.59 (t, *J*=6.4 Hz, 1H), 7.76(d, *J*=15.2 Hz, 1H), 7.92 (d, *J*=15.2 Hz, 1H), 7.98(t, *J*=7.6 Hz, 1H), 8.10 (d, *J*=7.6 Hz, 1H), 8.69 (d, *J*=4.8Hz, 1H). ^{13}C-NMR (d_6-acetone, 150 MHz): δ=119.47, 126.18, 127.35, 129.89, 130.39, 133.70, 135.64, 138.71, 149.99, 151.24, 157.03, 158.25, 160.53, 186.12. IR (KBr, cm^{-1}): 3448(w), 3070(w),

1644(m), 1574(s), 1491(s), 1439(vs), 1378(m), 1287(m), 1048(m), 757(m), 699(s). MALDI-TOF: *m/z*, *cal*: 382.11, found: 382.29 [M^+].

OC-0: M.p.= 114 ^oC. ^1H-NMR (d_6-acetone, 400 MHz, ppm) δ =1.33 (t, *J*= 6.8 Hz, 6H), 4.03 (q, *J*= 6.8 Hz, 4H), 6.08 (d, *J*= 4.0 Hz, 1H), 6.99 (m, 5H), 7.26 (d, *J*=8.8 Hz, 4H), 7.35 (d, *J*=4.0 Hz, 1H), 7.49(m, 2H), 7.59(t, *J*=7.2 Hz, 1H), 7.78 (d, *J*=14.8 Hz, 1H), 8.00 (d, *J*=4.0 Hz, 2H). ^{13}C-NMR (d_6-DMSO, 150 MHz): δ=14.62, 63.28, 109.65, 114.04, 115.51, 125.90, 127.01, 127.99, 128.58, 132.38, 136.47, 138.10, 138.85, 156.59, 160.05, 187.63. IR (KBr, cm^{-1}): 3429(w), 3101(w), 3050(w), 2981(w), 2928(w), 2869(w), 1645(m), 1564(m), 1505(s), 1454(vs), 1386(m), 1302(m), 1240(s), 1175(m), 1045(m), 1013(m), 821(m). MALDI-TOF: *m/z*, *cal*: 469.17, found: 469.33 [M^+].

OC-1: M.p.=125 ^oC. ^1H-NMR (d_6-acetone, 400 MHz, ppm) δ=1.34 (t, *J*= 6.8 Hz, 6H), 4.04 (q, *J*= 6.8 Hz ,6H), 6.08 (d, *J*= 4.4 Hz,1H), 6.98 (d, *J*=8.8 Hz, 4H), 7.29 (d, *J*=8.8 Hz, 4H), 7.36 (d, *J*=4.4 Hz, 1H), 7.46(d, *J*=15.2Hz, 1H), 7.62(m, 1H), 7.86 (d, *J*=15.2 Hz, 1H), 8.01 (m, 2H), 8.70 (d, *J*=4.8 Hz, 1H). ^{13}C-NMR (d_6-DMSO, 150 MHz): δ=13.90, 62.60, 115.50, 115.56, 117.36, 119.23, 127.10, 127.69, 137.85, 138.62, 139.10, 148.86, 154.86, 156.37, 160.38, 165.15, 188.22. IR (KBr, cm^{-1}): 3432(w), 3048(w), 2978(w), 2928(w), 2875(w), 1647(m), 1562(s), 1507(s), 1443(vs), 1383(m), 1333(m), 1241(s), 1174(m), 1023(m), 827(m). MALDI-TOF: *m/z*, *cal*: 470.17, found: 469.73 [M^+].

OC-2: M.p.=162 ^oC. ^1H-NMR (d_6-DMSO, 400 MHz, ppm) δ=1.33 (t, *J*= 7.2 Hz, 6H), 4.03 (q, *J*= 7.2 Hz, 4H), 6.08 (d, *J*= 4.4 Hz,1H), 6.98 (d, *J*=8.0 Hz, 4H), 7.03 (s, 1H), 7.28 (d, *J*=8.0 Hz, 4H), 7.40 (d, *J*=4.4 Hz, 1H), 7.51 (dd, 1H), 7.83 (d, *J*=14.8 Hz, 1H), 8.35 (d, *J*=8.0 Hz, 1H), 8.74 (d, *J*=4.8 Hz, 1H), 9.15 (s, 1H). ^{13}C-NMR (d_6-DMSO, 150 MHz): δ=14.62, 63.29, 113.48, 115.53, 117.36, 125.56, 127.13, 135.52, 138.68, 149.02, 156.73, 160.95, 186.58. IR (KBr, cm^{-1}): 3463(w), 3043(w), 2977(w), 2910(w), 2878(w), 1642(m), 1573(s), 1505(s), 1444(vs), 1380(m), 1329(m), 1277(s), 1047(s), 806(m). MALDI-TOF: *m/z*, *cal*: 470.17, found: 470.54 [M^+].

S3. Results

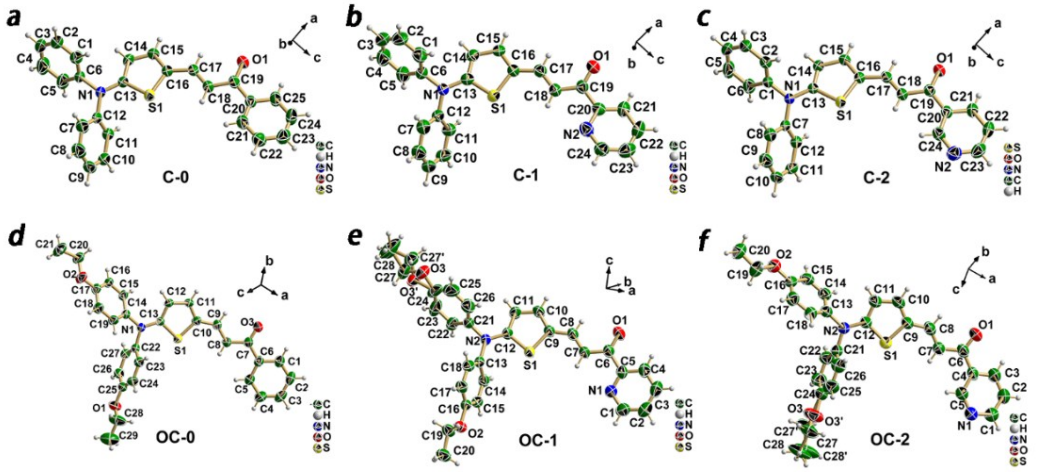

Figure S1. The crystal structure of **C-0**, **C-1**, **C-2**, **OC-0**, **OC-1** and **OC-2**, with atom labels and 50% probability displacement ellipsoids for non-H atoms.

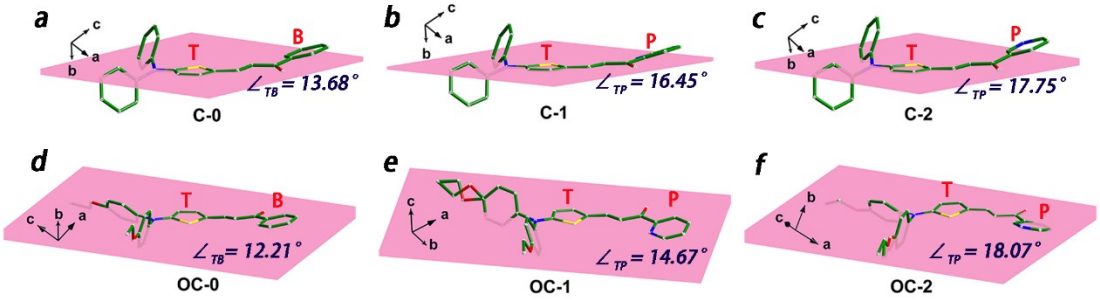

Figure S2. Planarity sketch of **C-0**, **C-1**, **C-2**, **OC-0**, **OC-1** and **OC-2**; H atoms are omitted for clarity

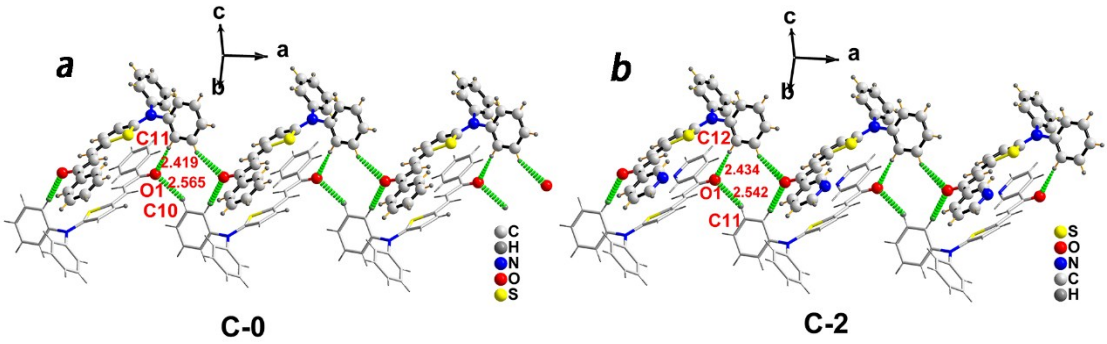

Figure S3. Hydrogen bonds of **C-0** and **C-2** (green dash bonds)

Table S1. Crystal data and structure refinement for **C-0**, **C-1**, **C-2**, **OC-0**, **OC-1** and

						OC-2
Comps	**C-0**	**C-1**	**C-2**	**OC-0**	**OC-1**	**OC-2**
CCDC No.	1407843	1434101	964082	1407844	1407845	1407846
Empirical formula	$C_{25}H_{19}NOS$	$C_{24}H_{18}N_2OS$	$C_{24}H_{18}N_2OS$	$C_{29}H_{27}NO_3S$	$C_{28}H_{26}N_2O_3S$	$C_{28}H_{26}N_2O_3S$
Formula weight	381.48	382.46	382.46	469.58	470.57	470.57
Temperature	296(2) K	293(2) K	296(2) K	296(2) K	296(2) K	293(2) K
Wavelength	0.71073 Å	0.71069 Å	0.71069 Å	0.71073 Å	0.71073 Å	0.71073 Å
Crystal system	$P2_1/n$	$P2_1/c$	$P2_1/c$	$P\bar{1}$	$P\bar{1}$	$P\bar{1}$
space group	monoclinic	monoclinic	monoclinic	triclinic	triclinic	triclinic
a/Å	11.145(6)	10.931(5)	10.976(5)	5.5078(9)	7.406(5)	9.185(4)
b/Å	18.243(9)	18.464(5)	18.029(5)	13.846(2)	11.831(9)	11.757(5)
c/Å	9.722(5)	9.657(5)	9.697(5)	16.264(3)	14.142(10)	12.715(5)
α/(°)	90	90	90	85.220(2)	89.231(9)	100.884(6)
β/(°)	90.995(6)	90.000(5)	90.728(5)	84.223(2)	81.249(9)	101.591(5)
γ/(°)	90	90	90	85.091(2)	89.949(9)	106.300(5)
V/Å^3	1976.4(18)	1949.1(14)	1918.7(14)	1226.0(3)	1224.6(15)	1246.3(8)
Z	4	4	4	2	2	2
D_c/Mg m^{-3}	1.282	1.303	1.324	1.272	1.276	1.254
μ/mm^{-1}	0.179	0.183	0.186	0.163	0.164	0.162
F(000)	800	800	800	496	496	496
Final R indices [I>2σ(I)]	R_1 = 0.0434, wR_2 =0.1226	R_1 = 0.0725, wR_2 = 0.1823	R_1 = 0.0388, wR_2 = 0.1170	*R_1= 0.0481, wR_2=0.1399*	R_1 = 0.0421, wR_2 = 0.0994	R_1 = 0.0530, wR_2 = 0.1083
Goodness-of-fit on F^2	0.889	0.908	0.947	1.036	0.970	0.931

Table S2. Selected bond distances (Å) and angles (°) for **C-0**, **C-1**, **C-2**, **OC-0**, **OC-1** and **OC-2**

		C-0	
C(6)-N(1)	1.438(3)	C(12)-N(1)-C(6)	119.34(17)
C(13)-N(1)	1.387(3)	C(13)-N(1)-C(6)	117.95(17)
C(13)-S(1)	1.739(2)	C(13)-N(1)-C(12)	122.33(17)
C(17)-C(18)	1.332(3)	C(13)-S(1)-C(16)	91.65(10)
C(19)-O(1)	1.229(2)	C(18)-C(19)-C(20)	119.78(19)
C(20)-C(21)	1.379(3)	C(25)-C(20)-C(19)	118.3(2)
C(16)-C(17)	1.435(3)		
		C-1	
C(6)-N(1)	1.436(7)	C(13)-N(1)-C(12)	122.7(4)
C(13)-N(1)	1.397(7)	C(12)-N(1)-C(6)	117.2(4)
C(13)-S(1)	1.723(5)	C(13)-N(1)-C(6)	119.7(4)
C(17)-C(18)	1.334(7)	C(13)-S(1)-C(16)	92.3(2)

C(19)-O(1)	1.227(6)	C(18)-C(19)-C(20)	119.5(5)
C(20)-N(2)	1.340(6)	C(21)-C(20)-C(19)	121.2(5)
C(16)-C(17)	1.428(7)		
		C-2	
N(1)-C(13)	1.380(3)	C(13)-N(1)-C(7)	122.32(17)
N(1)-C(1)	1.439(3)	C(13)-N(1)-C(1)	117.96(16)
S(1)-C(13)	1.741(2)	C(7)-N(1)-C(1)	119.03(16)
C(18)-C(17)	1.333(3)	C(13)-S(1)-C(16)	91.72(9)
O(1)-C(19)	1.226(2)	C(18)-C(19)-C(20)	119.82(18)
N(2)-C(24)	1.343(3)	C(21)-C(20)-C(19)	118.52(19)
C(16)-C(17)	1.431(3)		
		OC-0	
C(25)-O(1)	1.375(3)	C(5)-C(6)	1.374(3)
C(28)-O(1)	1.445(4)	C(17)-O(2)-C(20)	118.0(2)
C(14)-N(1)	1.434(3)	C(13)-N(1)-C(14)	122.61(18)
C(13)-N(1)	1.369(3)	C(13)-N(1)-C(22)	119.98(17)
C(13)-S(1)	1.744(2)	C(14)-N(1)-C(22)	117.29(17)
C(8)-C(9)	1.335(3)	C(13)-S(1)-C(10)	91.71(10)
C(7)-O(3)	1.232(3)	C(1)-C(6)-C(7)	118.8(2)
C(9)-C(10)	1.426(3)		
		OC-1	
C(16)-O(2)	1.364(2)	C(5)-N(1)	1.331(3)
C(19)-O(2)	1.433(3)	C(16)-O(2)-C(19)	117.20(15)
C(12)-N(2)	1.371(2)	C(12)-N(2)-C(13)	122.32(16)
N(2)-C(21)	1.437(2)	C(12)-N(2)-C(21)	119.19(16)
C(12)-S(1)	1.733(2)	C(13)-N(2)-C(21)	118.09(15)
C(7)-C(8)	1.337(3)	C(12)-S(1)-C(9)	91.56(10)
C(6)-O(1)	1.225(2)	C(4)-C(5)-C(6)	119.3(2)
C(8)-C(9)	1.418(3)		
		OC-2	
C(16)-O(2)	1.369(3)	C(5)-N(1)	1.338(4)
C(19)-O(2)	1.419(3)	C(16)-O(2)-C(19)	117.7(3)
C(13)-N(2)	1.432(4)	C(12)-N(2)-C(13)	122.1(2)
C(12)-N(2)	1.369(4)	C(12)-N(2)-C(21)	120.8(2)
C(12)-S(1)	1.728(3)	C(13)-N(2)-C(21)	116.9(2)
C(7)-C(8)	1.342(4)	C(12)-S(1)-C(9)	92.03(15)
C(6)-O(1)	1.226(3)	C(3)-C(4)-C(6)	119.1(3)
C(8)-C(9)	1.422(4)		

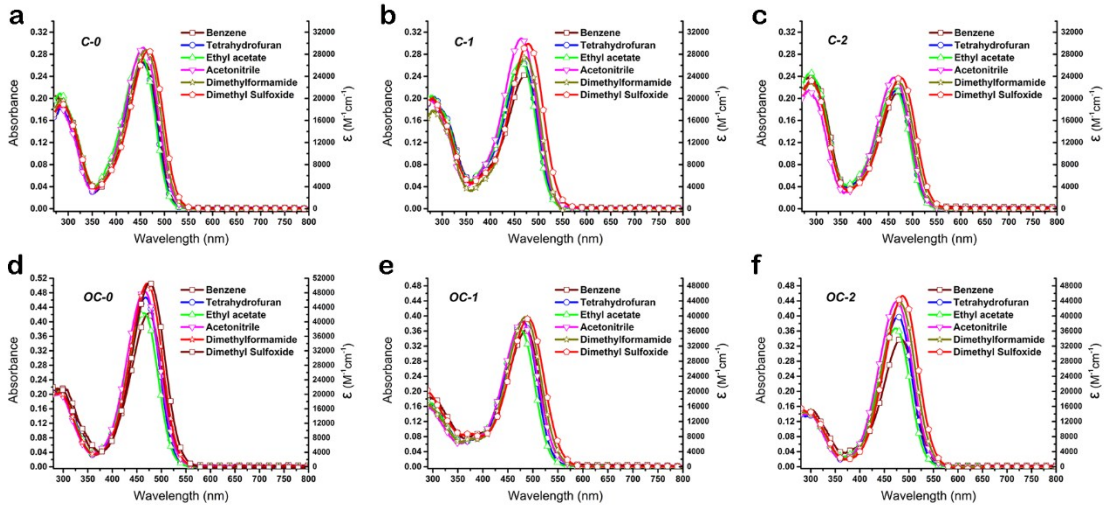

Figure S4. UV-vis spectra of **C-0**, **C-1**, **C-2**, **OC-0**, **OC-1** and **OC-2** in different solvents (1.0×10^{-5} mol/L).

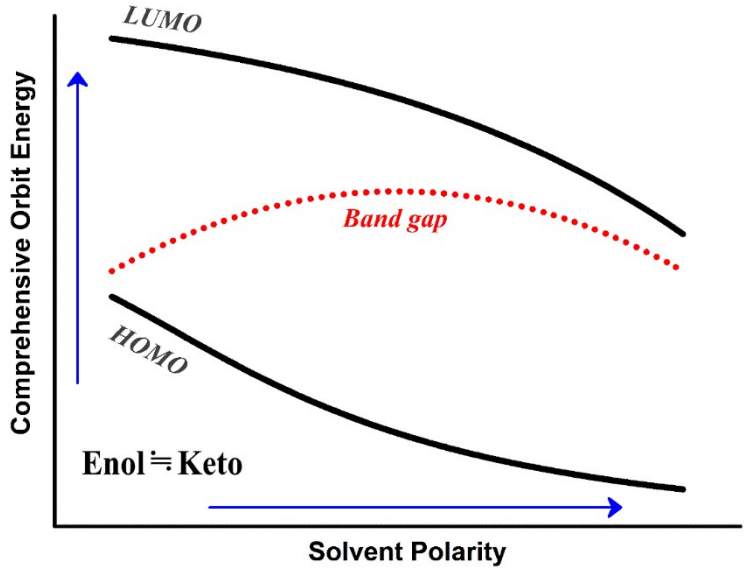

Figure S5. An inferred illustration for the changes of molecular orbital energy at ground/excited state and relevant bang gap caused by polarity of different solvents.

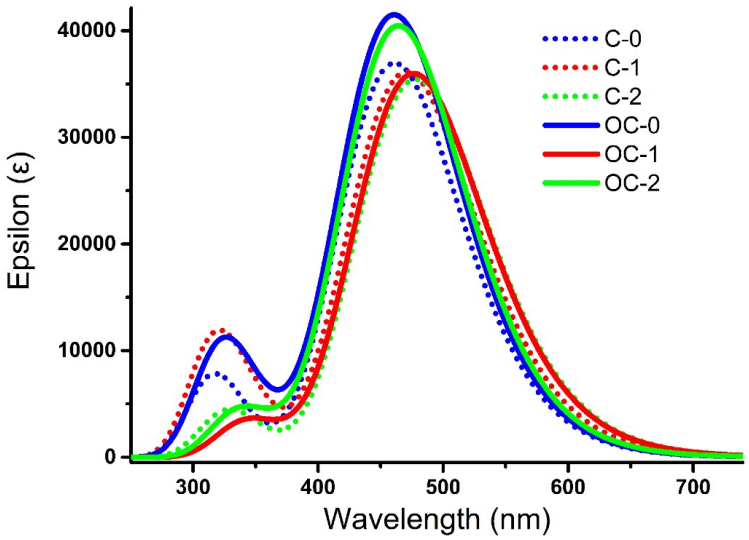

Figure S6. The linear absorption spectra of **C-0**, **C-1**, **C-2**, **OC-0**, **OC-1** and **OC-2** in THF calculated by the TD-B3LYP method with 6-311+G(d) basis sets in THF.

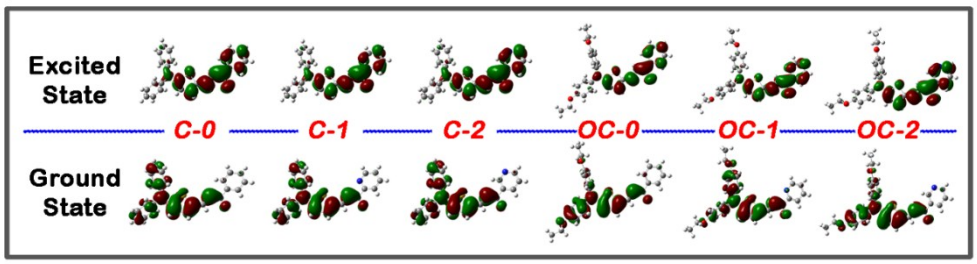

Figure S7. The transition molecular orbital diagrams for **C-0**, **C-1**, **C-2**, **OC-0**, **OC-1** and **OC-2** in THF using the TD-B3LYP method with 6-311+G(d) basis sets.

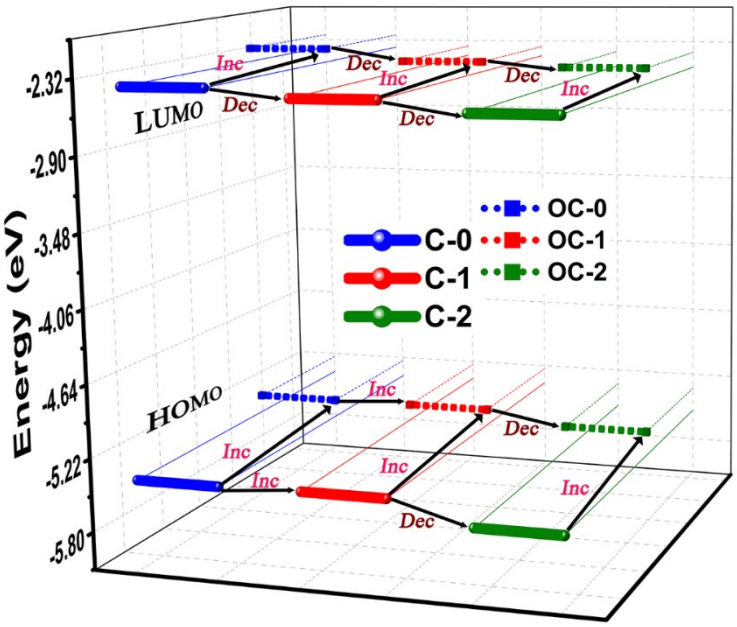

Figure S8. 3D illustration for the changes of molecular orbital energy at

ground/excited state in THF caused by different terminal electron-withdrawing/donating groups.(*Inc* refers to increase, and *Dec* refers to decrease)

Table S3. The influence of tunable electron- donating/withdrawing groups on the energy of LUMO and HOMO

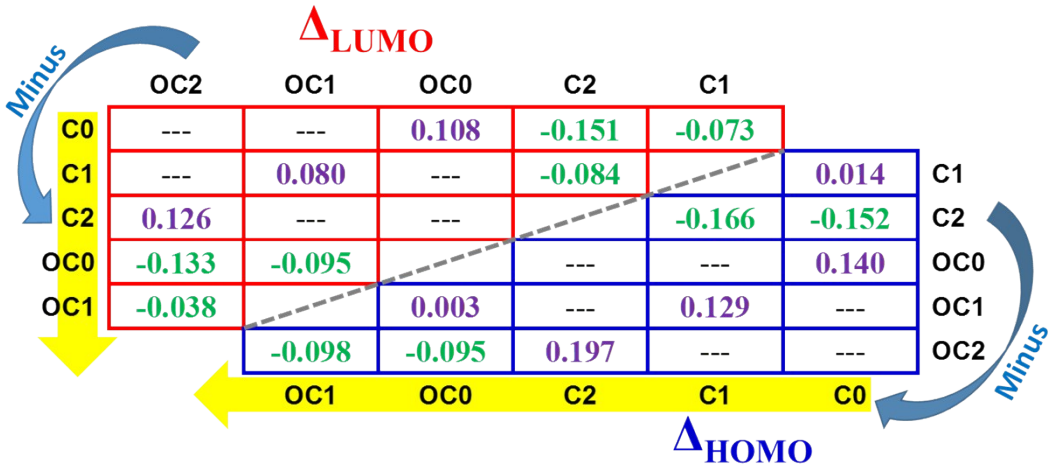

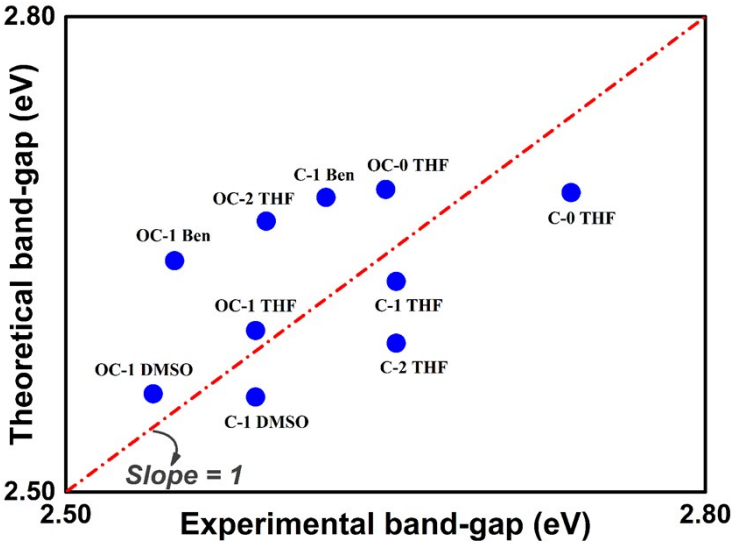

Figure S9. The correlation between the theoretical and experimental band-gap.

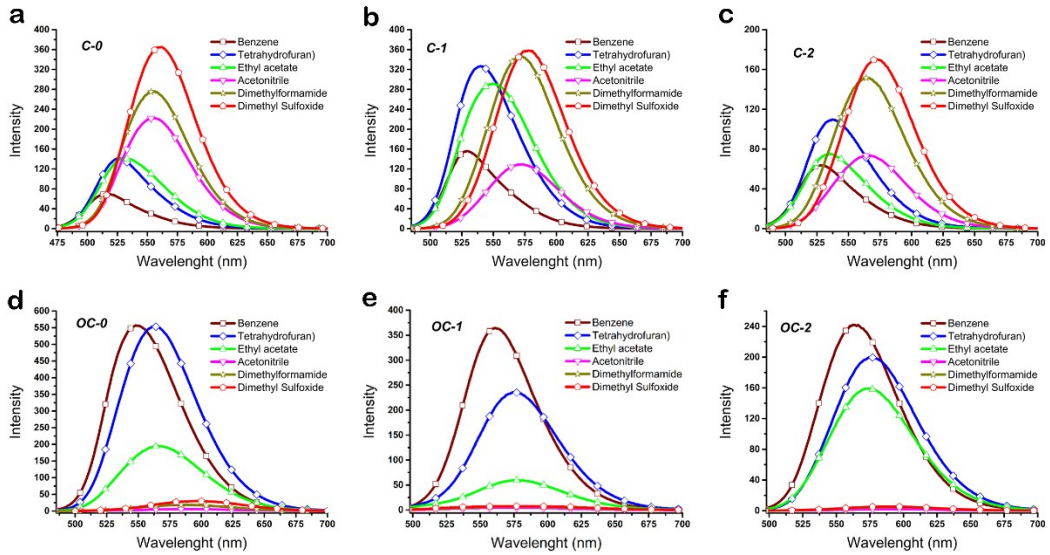

Figure S10. The OPEF spectra of **C-0**, **C-1**, **C-2**, **OC-0**, **OC-1** and **OC-2** in different solvents (1.0×10^{-5} mol/L).

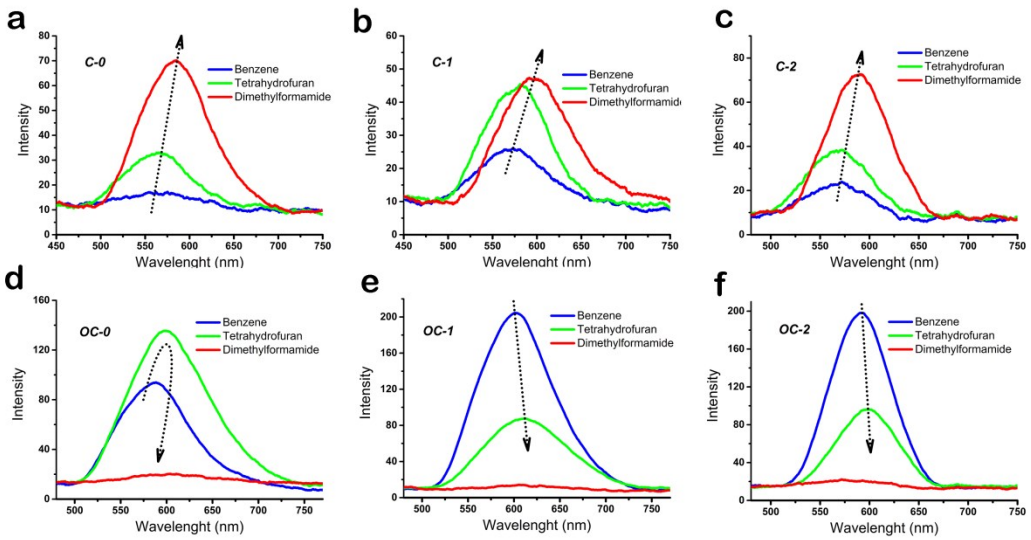

Figure S11. The 2PEF emission band of **C-0**, **C-1**, **C-2**, **OC-0**, **OC-1** and **OC-2** excited at the optimum wavelength in three different solvents (1.0×10^{-3} mol/L).

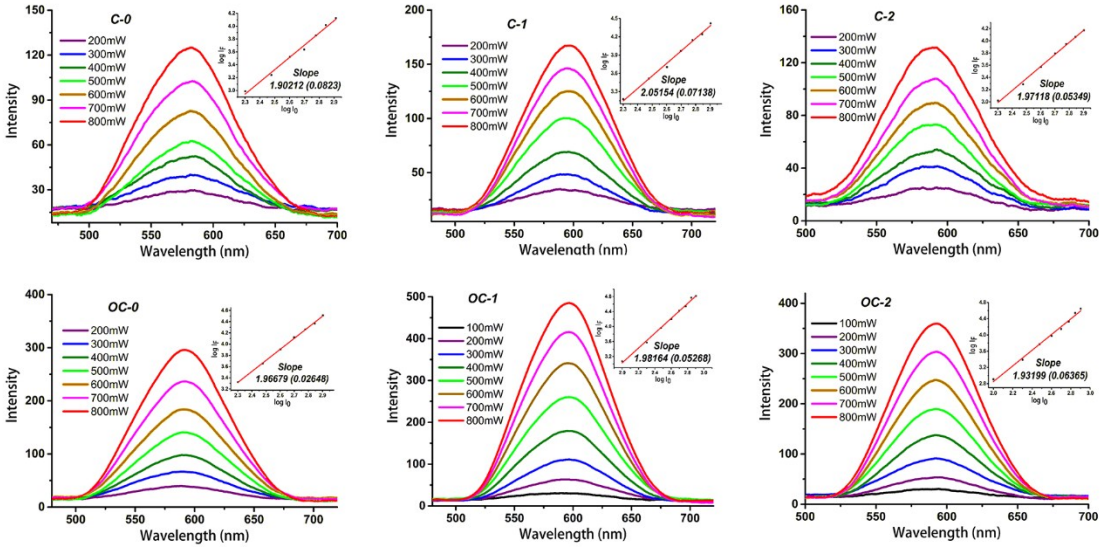

Figure S12. The 2PEF spectra of **C-0**, **C-1**, **C-2**, **OC-0**, **OC-1** and **OC-2** excited by the different input laser power at the optimum wavelength in the optimum solvent (1.0×10^{-3} mol/L), the inset shows the two-photon absorption verification of those chalcone which I_{in} and I_{out} represent the input laser power and output fluorescence, respectively.

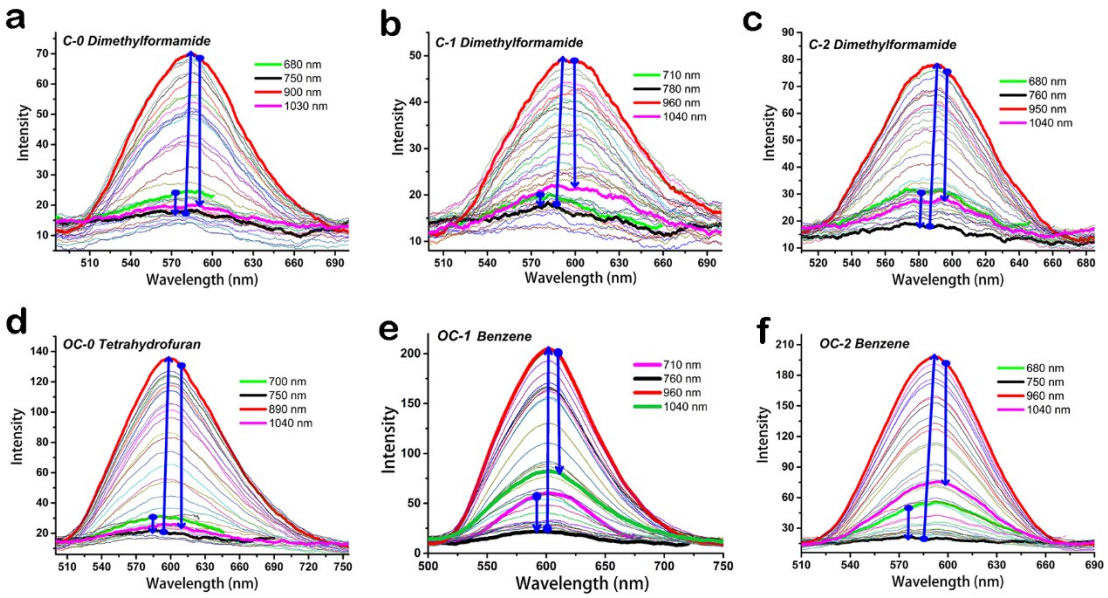

Figure S13. The 2PEF spectra of **C-0**, **C-1**, **C-2**, **OC-0**, **OC-1** and **OC-2** excited at the different wavelength in the optimum solvent (1.0×10^{-3} mol/L).

Reference

1 G. Sheldrick, *Shelxl-97, Program for Crystal Structure Refinement*; University of Göttingen, Germany, **1997**.

2 G. Sheldrick, Shelxs-97, Program for X-Ray Crystal Structure Solution. University of Göttingen, Germany: 1997.

3 G. Trucks; H. Schlegel; G. Scuseria; M. Robb; J. Cheeseman; J. Montgomery Jr; T. Vreven; K. Kudin; J. Burant and J. Millam, *Gaussian 03*. In *Revision B. 04*, Gaussian, Inc. Pittsburgh PA: **2003**.
4 J. Demas and G. A. Crosby, *J Phys Chem*, 1971, **75**, 991-1024.
5 N. S. Makarov; M. Drobizhev and A. Rebane, *Opt Express*, 2008, **16**, 4029-4047.
6 C. Xu and W. W. Webb, *J Opt Soc Am B*, 1996, **13**, 481-491.
7 J. H. Strickler and W. Ww., *Opt Lett*, 1991, **16**.
8 R. Cammi; M. Cossi and J. Tomasi, *J Chem Phys*, 1996, **104**.
9 Y. R. Shen, *New York, Wiley-Interscience, 1984, 575 p.*, 1984, **21**, 400.
10 J. Olsen and P. Jorgensen, *J Chem Phys*, 1985, **82**, 3235-3264.
11 Gaussian 09, References in http://www.gaussian.com.
12 Dalton, a molecular electronic structure program, see http://daltonprogram.org.